Vol. 69: 129–141, 2016
doi: 10.3354/cr01395

CLIMATE RESEARCH
Clim Res

Published online June 27

Effects of climate change on the yield of winter wheat in the eastern Mediterranean and Middle East

K. Constantinidou[1,*], P. Hadjinicolaou[1], G. Zittis[1], J. Lelieveld[1,2]

[1]Energy Environment and Water Research Center, The Cyprus Institute, 1645 Nicosia, Cyprus
[2]Department of Atmospheric Chemistry, Max Plank Institute for Chemistry, 55020 Mainz, Germany

ABSTRACT: Warming and drying in the eastern Mediterranean and the Middle East (EMME) associated with climate change may have consequences for humans and ecosystems, including agriculture. Agriculture can be directly affected through meteorological conditions that influence crop growth and yield. Here we explored changes in the yield of durum (winter) wheat *Triticum tirgidum* in the EMME region caused by projected changes in thermal and hydrological conditions, employing the agro-ecological zones (AEZ) methodology. The climate input was obtained from simulations by the PRECIS regional climate model over the EMME domain at 25 km resolution, driven by a range of IPCC emissions scenarios for the 21st century. For the crop yield calculation, we used 2 steps of the biomass calculation from the AEZ methodology by calculating crop yield potentials with regard to temperature, solar radiation and evapotranspiration regimes. Our results showed that for the recent past, the highest wheat yields are found in the Fertile Crescent and the coastal areas of eastern Mediterranean Europe. The former region is projected to be negatively affected by the additional heat due to climate warming, while in the latter region yield gains may be expected. Our implementation of the AEZ methodology can be based on a range of climate data and can be applied to a number of crops, contributing to yield studies relevant for regional assessments of food security.

KEY WORDS: *Triticum tirgidum* · Yield · Agro-ecological zones methodology · Regional climate change · Eastern Mediterranean – Middle East

1. INTRODUCTION

The region of the eastern Mediterranean and the Middle East (EMME) is home to more than 350 million people in an area with a 2000 km radius, including large sea and desert areas. After many years of industrialization, rapid population growth and extensive land use changes that have shaped the region, it has additionally become a global climate change 'hot spot'; trends in climate conditions, documented by observations in the EMME, indicate a strong temperature increase and precipitation decrease during the last decades of the 20th century (Tanarhte et al. 2012). This warming and drying is projected to intensify in the 21st century and may have major consequences for society and natural ecosystems (Lelieveld et al. 2012). One of the sectors that could be adversely impacted is agriculture, and the potential implications for food security may be critical for this region with increasing population, limited adaptive capacity (determined by economic resources, technology, information and skills, infrastructure, institutions, and equity; see e.g. Grasso & Feola 2012) and geopolitical sensitivities.

The EMME encompasses sub-regions that are very suitable for agriculture. Current climate conditions in the region allow for a large variety of crops, including C3 and C4 cereals, legumes and root crops (Leff et al. 2004, Lelieveld et al. 2012).

Wheat is among the 'big 3' cereal crops, with over 600 Mt harvested annually in the world (Shewry et al. 2009). In 2009, 226 million ha were sown to wheat;

*Corresponding author: k.constantinidou@cyi.ac.cy

yielding 685 Mt of grain from about 3 t ha^{-1} (Asseng et al. 2012; also see http://faostat.fao.org/). Wheat is a cool-season crop originating in the Fertile Crescent in the EMME while it is now widely spread around the world. It can be grown in a range of climatic conditions, from arctic and humid regions to tropical highlands and from below sea level in the Dutch Polders to 4500 m altitude. The growing conditions are very diverse, not only because of the variable climatic regions and altitudes, but also because of differences in soil types and crop management.

Durum wheat *Triticum tirgidum* is regarded as one of the oldest cultivars of winter wheat. Durum originates in the eastern Mediterranean and has been cultivated in this region for the last 12 millennia (Key 2005). Whilst farming has spread globally, the durum wheat grown in the Mediterranean basin is of premium quality and accounts for ~60% of the global total production (Lidon et al. 2014). Products of durum wheat are key components of the staple diet in countries located in the Mediterranean basin. It is usually processed into semolina, which is used to make couscous, pasta, flat breads, bulgur and other products. Durum is one of the highest-priced grains traded on the world market, mostly as bread wheat and pasta (ICARDA 2001). The main environmental constraints limiting the production of durum wheat in this region are drought and temperature extremes, with productivity ranging from 0 to 6 t ha^{-1} (Nachit & Elouafi 2004). In relatively dry countries like Syria, the average yield is about 2.7 to 3 t ha^{-1} (which can vary in the range of 1 to 7 t ha^{-1} in some locations; ICARDA 2001).

Weather variations and climate variability have an impact on crop yields (Ciais et al. 2005, Iizumi et al. 2014), while long-term climate change also affects the quantity and quality of crop production through processes driven by sunlight, temperature, water and carbon dioxide levels (Olesen & Bindi 2002). Several studies have projected crop yields under changing mean and extreme climate conditions with a variety of climate models, emission scenarios and crop simulation models (e.g. Iglesias et al. 2000, Moriondo et al. 2011, Sen et al. 2012, Naresh Kumar et al. 2014, Vanuytrecht et al. 2014). These particular studies projected crop yield vulnerability at the country level by focusing on specific locations, representative of maximum production, and applying crop simulation models with detailed soil and management data.

Assessments of climate change impacts on agriculture and analysis of yield gap, (the difference between the potential yield of a crop and its actual production), offer useful knowledge towards sustainable intensification or/and diversification of agriculture for the optimization of food supply, but require calculations over climatically homogeneous zones (Van Ittersum et al. 2013, Van Wart et al. 2013). The Agricultural Model Intercomparison and Improvement Project seeks, among its several objectives, to develop methods to allow site/point analyses to be scaled up to larger regions (Rosenzweig et al. 2013). Recently, Rosenzweig et al. (2014) presented the results from 7 global gridded crop models (site-based, ecosystem and agro-ecological zone models) where crop yields of wheat were projected to increase in south-east Europe and decrease in North Africa and the Levant by the end of this century.

We focus on the EMME, a climate change hot spot facing multiple challenges where wheat is an important staple food, and follow a framework of the analysis of large-scale shifts in cropping zones by implementing the agro-ecological zones (AEZ) methodology developed by the Food and Agriculture Organization of the United Nations (FAO) and the International Institute for Applied Systems Analysis (IIASA) (Fischer et al. 2002, Teixeira et al. 2013). It provides a spatial inventory and database of land resources and crop production potentials. This land resources inventory is used for specified management conditions and climate input, to assess the suitability of crops and to quantify expected production of cropping activities relevant in the specific agro-ecological context.

Here we adopted the AEZ methodology and combined it with projections, for the first time as far as we know, from a regional climate model (RCM), the Hadley Centre PRECIS RCM, to derive yield potentials of winter wheat in the EMME region, spatially gridded at a resolution of 25 × 25 km. For the winter type of wheat that we address, we assumed a growth cycle duration of 180 d (sowing date 1 November and harvesting day 30 April). This crop calendar was selected because in the EMME region, wheat is usually cultivated during this period of the year, the beginning of which also coincides with the start of the wet season (Sacks et al. 2010).

2. CLIMATE DATA

The biomass model used for calculation of potential yield requires as climatic input mean temperature and incoming shortwave solar radiation data. Minimum and maximum daily temperature, mean daily relative humidity and wind speed are needed for calculations of the second step in this model, which

results in water-limited yields. These are obtained from simulations performed by the PRECIS ('Providing REgional Climates for Impacts Studies') regional climate model, developed by the UK Met Office Hadley Centre. This RCM uses the same formulation of the climate system as its parent global model HadCM3 (Collins et al. 2006), which also provides boundary conditions from simulations driven by the 'optimistic' B2 scenario, the intermediate A1B scenario and the 'pessimistic' A2 scenario, based on the IPCC Special Report on Emissions Scenarios (SRES) (Nakicenovic et al. 2000).

PRECIS was applied from 1950–2099, forced by the A1B scenario over a domain covering the EMME region at a horizontal resolution of 0.22° (~25 km) and 19 vertical levels. The domain boundaries are 22–44° N and 13–55° E. The results from the simulation presented here have been evaluated extensively and used in EMME climate change impact studies and previous assessments (Chenoweth et al. 2011, Lelieveld et al. 2012, Zittis et al. 2014). We also included results from three 30 yr PRECIS simulations driven by a slightly different global model HadCM3 version, i.e. 1 baseline simulation for 1961–1990 and 2 future simulations for 2071–2099 (for the B2 and A2 emission scenarios, see Zittis et al. 2015 for details).

The data used are daily time series generated by the above simulations divided into 2 periods representing climate conditions of the 20th century past and future, i.e. end of the 21st century. The baseline (BL) period used as a reference is 1961–1990 and the future period (P3) is 2071–2099.

3. METHODOLOGY

Calculations of potential yields of winter wheat are made using the first step of the biomass and yield calculation model of the global AEZ (GAEZ) methodology developed by FAO and IIASA (Fischer et al. 2002, 2012; see http://webarchive.iiasa.ac.at/Research/LUC/GAEZv3.0/). It calculates the constraint-free crop yields, which reflect yield potentials with regard to temperature and radiation regimes prevailing in the relevant grid cells and are based on the eco-physiological model developed by Kassam (1977).

Firstly, a thermal suitability test is applied. This test is performed using the temperature profile requirements (Table 1 for winter wheat), i.e. crop-specific rules that take into account the crop growth cycle duration in different classes of mean daily temperatures. Temperature profiles are defined in terms of 9 classes of 'temperature ranges' (denoted by '*L*(1–9)' in Table A1 in Appendix 1) for days with average temperatures <–5°C, –5 to 0°C, …, 25 to 30°C and >30°C (at 5°C intervals) combined with the increasing (denoted by '*a*') and decreasing (denoted by '*b*') temperature trends within the growth cycle.

Table 1. Optimum and sub-optimum conditions for wheat *Triticum tirgidum* (Fischer et al. 2012). *La* and *Lb* are lengths of the pre- and post-dormancy period, respectively, *L6a/b* to *L1a/b* are temperature intervals (increasing/decreasing trends) 5–10, 10–15, 15–20, 20–25, 25–30, >30°C

Sub-optimum conditions	Optimum conditions
$L6a < 0.667 \times Lb$	$L6a < 0.5 \times Lb$
$L2a + L2b < 0.333 \times Lb$	$L2a + L2b < 0.333 \times Lb$
$L1 = 0$	$L1 = 0$
$L2b + L3b + L4b + L5b < 0.5 \times Lb$	$L2b + L3b + L4b + L5b < 0.5 \times Lb$
$L3b + L4b + L5b + L6b > La$	$L3b + L4b + L5b + L6b > La$

The potential crop calendar of each grid box of the domain is tested for the match of crop temperature profile requirements and prevailing temperature profiles. Temperature profile conditions are tested against optimum and sub-optimum requirements of winter wheat (Table 1; more detailed description in Appendix 1). We identified the lowest and highest temperatures, which can be characterized as lower (5°C) and upper (30°C) thresholds for the cultivation of winter wheat (*L*6, which corresponds to days with mean temperature of 5–10°C and *L*1 = 0, i.e. no days with average temperature above 30°C, as shown in Table 1). The calculation presented here is under rainfed conditions, because we consider only the growth cycle (*L*) for this type of wheat. When the conditions are satisfied, the grid box is considered suitable for cultivation of winter wheat; otherwise, the grid boxes are marked as non-suitable.

The suitability test is applied to each grid box of the domain for the 2 time periods in which the climate data have been subdivided. Subsequent potential yield calculations are made only for suitable grid boxes. The potential yield of the crop is affected by the intensity of input and management that is assumed to be applied. In the EMME region, intermediate level of input is the most appropriate choice. The farming system is partly market oriented; thus, production for subsistence and commercial sale is a management objective. Production is based on improved varieties, on manual labour based on hand tools and/or animal traction and some mechanization. It is of medium intensity, with some fertilizer application and chemical pest disease

and weed control, adequate fallows and some conservation measures.

All equations of the biomass and yield calculation model (AEZ methodology; Kassam 1977, Fischer et al. 2012) are transferred into a script in R^2 programming language (www.r-project.org/) in order to perform the calculations. A more detailed description is presented in Appendix 2.

Potential yield (Y_p) is estimated from net biomass (B_n) (dry matter) using the equation:

$$Y_p = H_i \times B_n \quad (1)$$

where H_i is the harvest index, i.e. proportion of the net biomass of a crop that is economically useful.

All crop-specific input parameters needed for calculations are the following: N: normal growth cycle duration (N = 180 d); LAI: leaf area index (LAI = 4); harvest index (H_i = 0.35) (Fischer et al. 2012); L: growth ratio of the maximum rate of gross biomass production (b_{gm}) at actual LAI to b_{gm} at LAI = 5 (L = 0.91) (Oldeman & Frére 1982). Following sensitivity calculations in order to assess the relative contribution of temperature and solar radiation in the potential yield (Y_p) estimation, we found that the effect of temperature is 2 orders of magnitude larger than that of solar radiation.

Under rainfed conditions, water stress is a very important limiting factor for the expected yields. Using the second step of the biomass and yield calculation model of the AEZ methodology (Fischer et al. 2002, 2012), a water-stress limiting factor (fc_2) is calculated next. First, water requirements for each grid cell are calculated by taking into account the specific water balance and actual evapotranspiration of each grid box.

The total water requirement of a crop without any water stress is assumed to be the crop-specific potential evapotranspiration (ET_m). ET_m is calculated in proportion to reference potential evapotranspiration (ET_o) (calculated by the Penman-Monteith equation), multiplied by crop and crop-stage specific parameters '*kc*'; these values of *kc* for different stages of crop development (shown in Fig. 1) are given as input parameters.

Yield reduction in response to water deficits is calculated as a function of the relationship between actual crop evapotranspiration ($\sum ET_a$, mm d^{-1}) and maximum crop evapotranspiration ($\sum ET_m$, mm d^{-1}), both accumulated within the 4 crop stages (details can be found in Appendix 2). This water-stress yield-reduction factor, derived for the 1961–1990 conditions, is shown in Fig. 2. It is evident that the effect of this factor is to reduce yields in most of the EMME domain, especially the southern part, due to the dry BL conditions.

Following the above mentioned calculation, the water-stress yield-reduction factor (fc_2) is then multiplied by the potential yield (Y_p) obtained from Eq. (1) to derive water-limited yield (Y_w) estimations as in the following equation:

$$Y_w = fc_2 \times Y_p \quad (2)$$

4. RESULTS

Fields of mean temperature, incoming shortwave radiation and evapotranspiration from PRECIS (for the B2, A1B and A2 emissions scenarios) are distinguished in 2 time periods (BL = 1961–1990, P3 = 2071–2099) and used here to calculate the potential yields of winter wheat in the EMME region.

Fig. 3 shows maps of changes in temperature simulated for the end of the century and each emission scenario, compared to the BL period. In all 3 scenarios, the model projects an increase in temperature between 2 and 6°C (P3 – BL) over the whole domain, as also demonstrated in previous studies based on the same climate projections (e.g. Lelieveld et al. 2012). The largest temperature increases tend to oc-

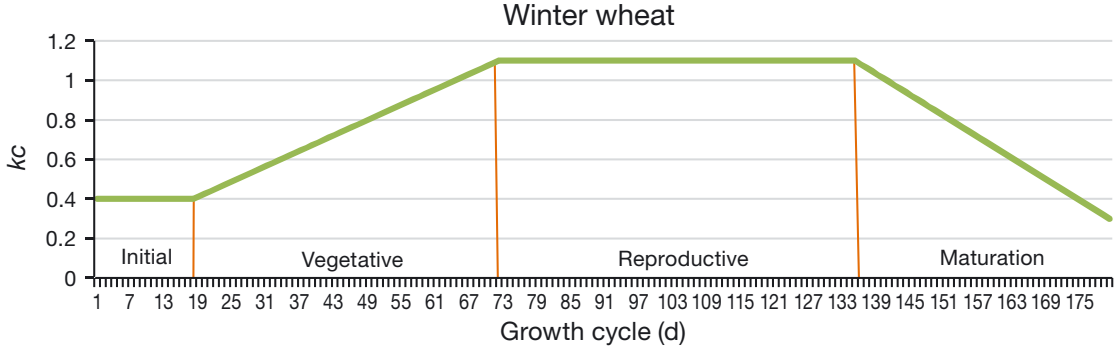

Fig. 1. Values of crop coefficients (*kc*) for winter wheat *Triticum tirgidum* developmental stages

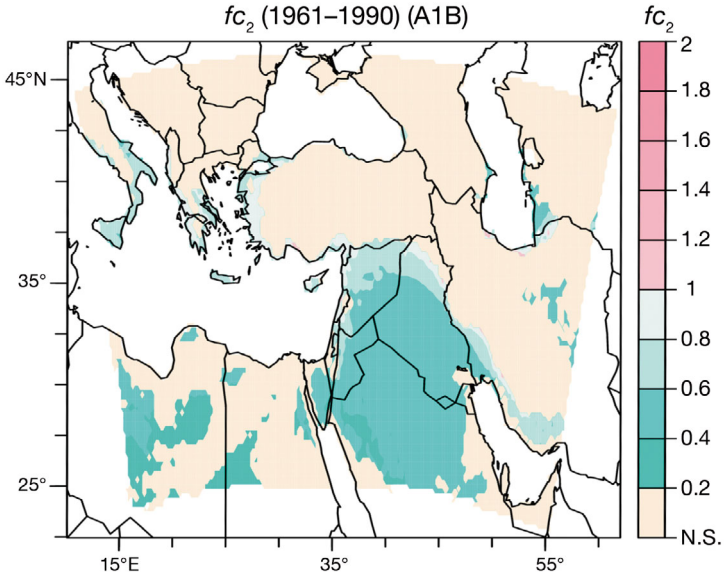

Fig. 2. Water-stress yield-reduction factor (fc_2) calculated for the baseline period driven by the intermediate A1B SRES scenario. N.S.: not suitable

cur over the main mountain ranges, which intensify according to the emission scenario. Solar radiation (Fig. 4) in the north-western part of the region shows an increasing tendency in the future, unlike the south-eastern part where it is decreasing. This spatial variation is the result of changes in cloud cover fraction (not shown), which are projected to reach −0.10 for Italy, the Balkans, Anatolia and the Levant (intensifying in the winter months), while they are positive (but small in the absolute sense, less than +0.05) in the southern and eastern parts of the domain (and mainly during the autumn and spring months).

The rate of water vapour lost through evapotranspiration in the future, as shown in Fig. 5, is about 1 to 2 mm d^{-1} in the northern and/or mountainous (covered by vegetation) part of the EMME domain according to the PRECIS simulation, while the values for the southern, desert areas are negligible. The projected changes in evapotranspiration are positive

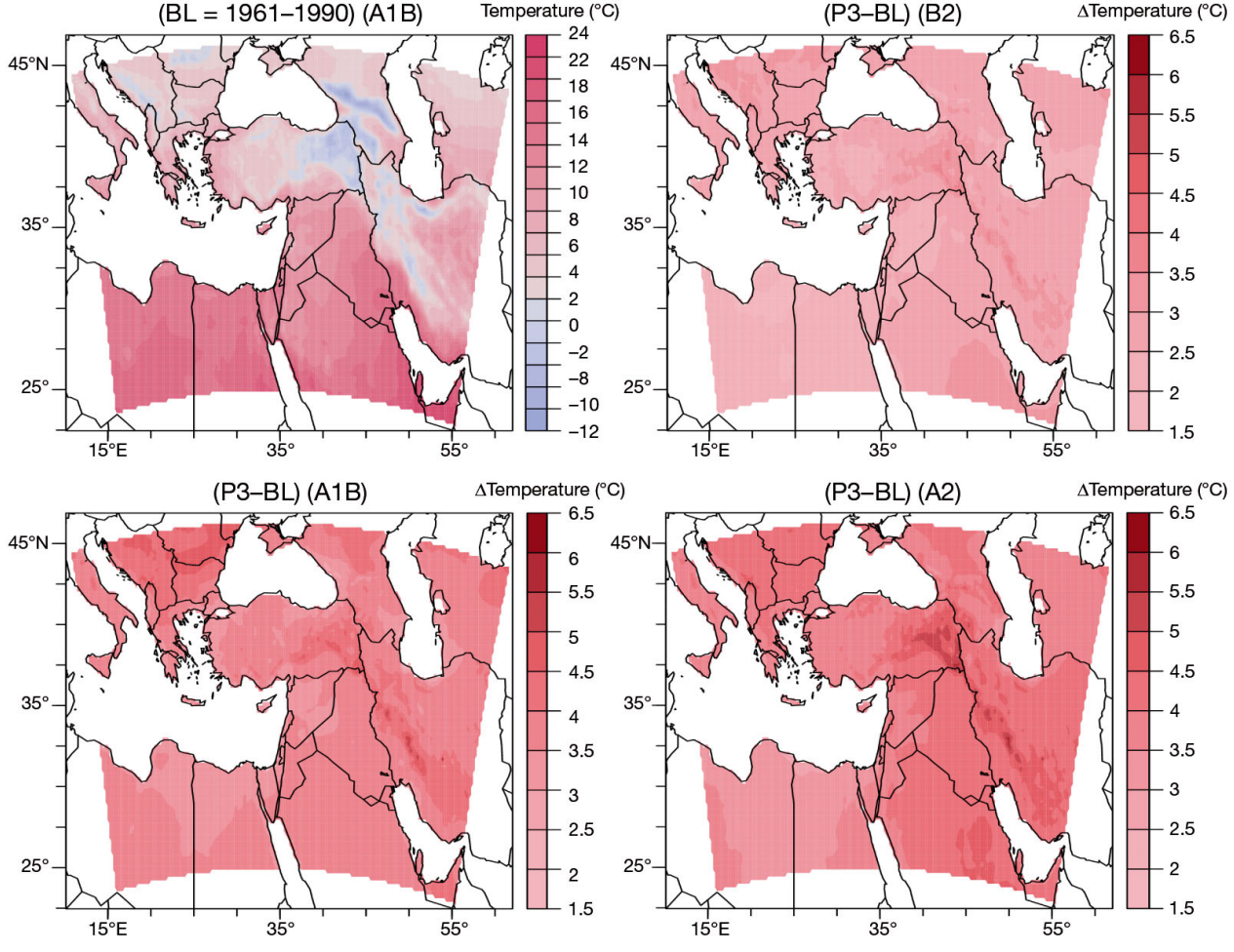

Fig. 3. November to April average temperature for the baseline (BL) period 1961–1990 for the A1B scenario and projected change for the future period (2071–2099; P3) relative to the BL for the B2, A1B and A2 SRES scenarios

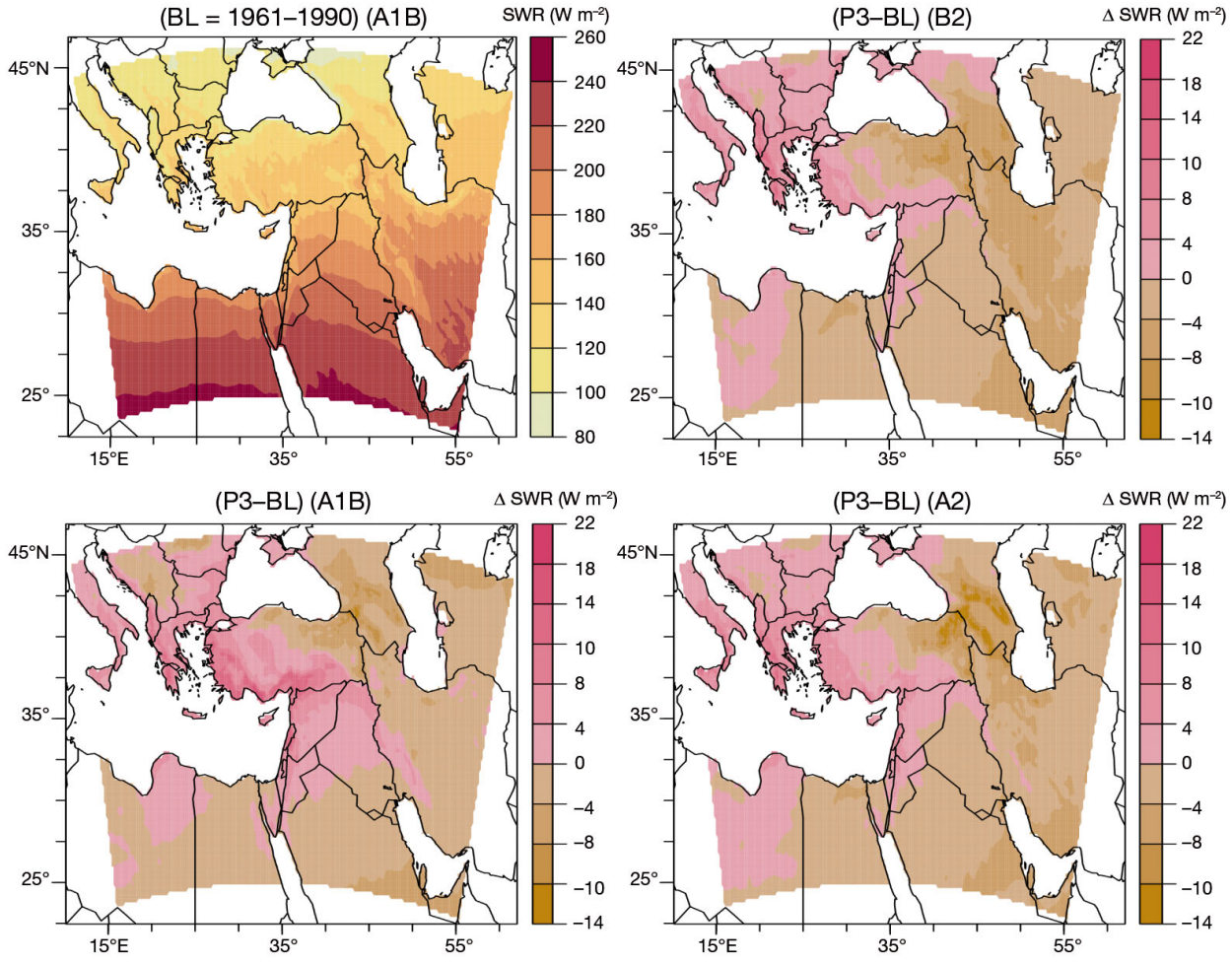

Fig. 4. November to April average shortwave radiation (SWR) for the baseline (BL) period 1961–1990 and projected change for the future period (2071–2099; P3) for B2, A1B and A2 SRES scenarios

in the northern and eastern parts of the domain and negative in the southern and western parts, driven by the differential warming (Fig. 3) as well as the availability of moisture (controlled by winter rainfall, see Fig. 3.2 in Zittis 2015).

Using the model fields of temperature and solar radiation, the whole domain is tested for suitability to grow winter wheat, i.e. if optimum and sub-optimum conditions (as shown in Table 1) are satisfied. This is done by testing whether temperature profile requirements and prevailing daily mean temperature regimes match in each grid box. Note that grid cells exceeding the lower and upper temperature thresholds of 5 and 30°C, respectively, for the growth of winter wheat (Table 1) are marked as non-suitable. Only the subsequent suitable fields are then used for the water-limited yield calculations, and the results are shown in Fig. 6.

The values calculated for the BL period can be compared with the literature and are within the indicated limits of actual durum production; as mentioned in the Introduction, the actual durum production in our area of interest ranges from 0 to 6 t ha^{-1} (Nachit & Elouafi 2004, Habash et al. 2009), and our calculations indicate a range for the whole domain of 2000 to 6500 kg ha^{-1} during the baseline period. Note also that despite the somewhat different absolute values for the yield between A1B and B2/A2 (due to non-identical climate data, as mentioned before), the spatial distribution of suitability among the 3 scenarios for the recent past is consistent. For 1961–1990, only the Fertile Crescent, the northern Arabian Peninsula and parts of Egypt and Libya appear to be suitable, with over 5000 kg ha^{-1} potential yield, and the coastal areas below 40° latitude with smaller yields between 3000 and 5000 kg ha^{-1}. The continental areas in the Balkans, Anatolia, Iran and the Caucasus do not appear suitable. In the future period, there is evidence of expanding suitability in the northern part of the region (mainland Italy, Greece, Anatolia, Azerbaijan, Turk-

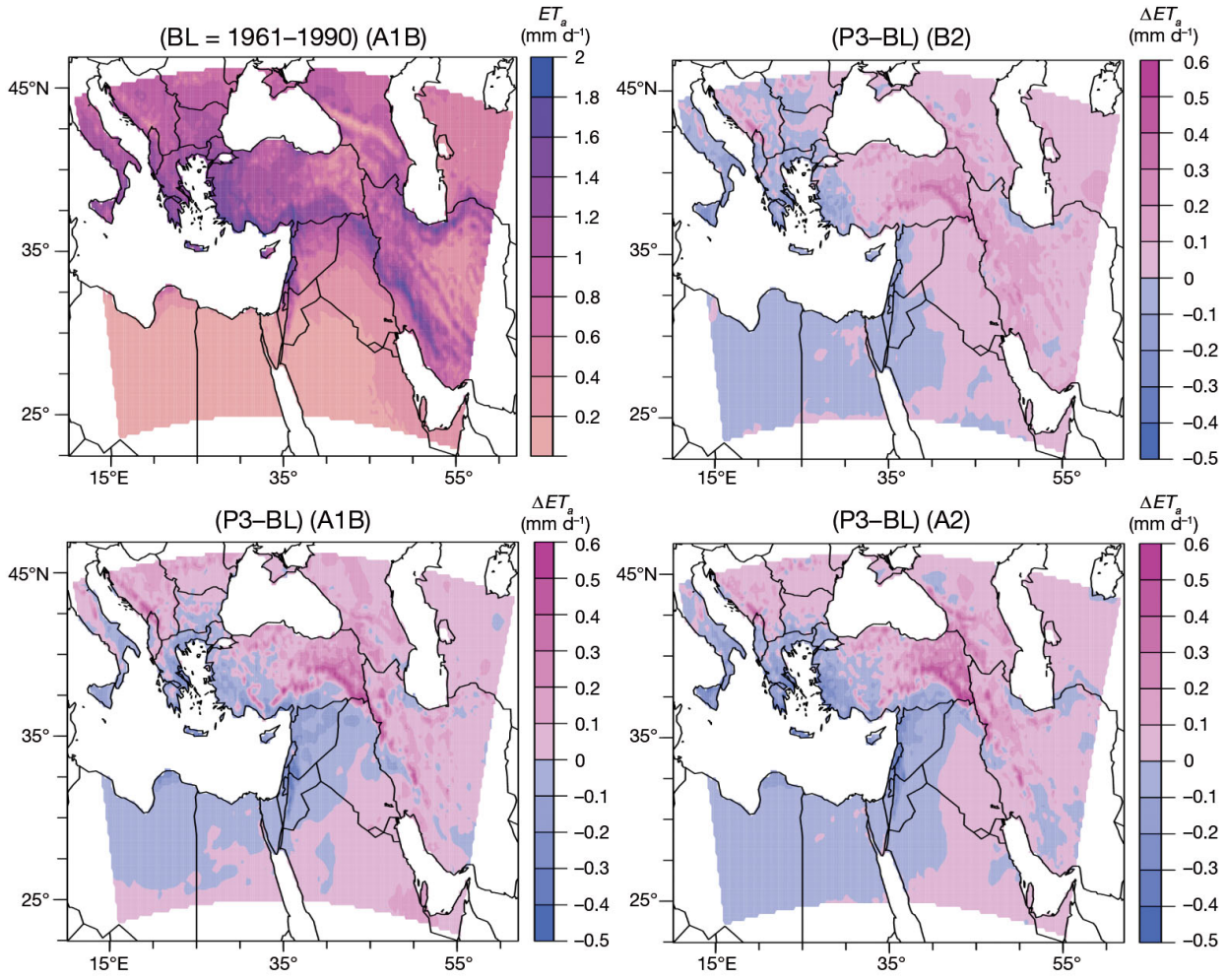

Fig. 5. November to April average actual evapotranspiration (ET_a) for the baseline (BL) period 1961–1990 and projected change for the future period (2071–2099; P3) for B2, A1B and A2 SRES scenarios

menistan, central Iran), reflecting the effects of the projected temperatures exceeding the threshold of around 5°C for the growth of wheat (as seen in Table 1 and in Fig. 2 of Luo 2011). Note that in the southern part of the domain, the projected warming, although less rapid than in the northern part (as seen in Fig. 3), leads to average November–April temperatures near 30°C and to a reduction in the potential yield area, as the temperature profile requirements are not met because the upper threshold of optimum conditions is surpassed. The affected areas include northern Africa, Sicily, Crete, Cyprus and parts of the Middle East, which will become, according to the calculations, unsuitable by the end of the century.

As mentioned in the Methodology section, water stress is a very important limiting factor for the estimated crop yield, cultivated under rainfed conditions. Fig. 7 shows the water-stress yield-reduction factor (fc_2) (its implementation determines the water-limited yield shown in Fig. 6) for the recent past and the future for all 3 emissions scenarios. During the BL period (1961–1990), the effect of the water requirement is to reduce the thermally-based potential yield (values of $fc_2 < 1$) over almost all of the suitable areas of the EMME domain, with the minor exceptions of Greece and the western coastlines of Italy and Turkey, where a slight enhancement is projected (values of fc_2 greater than 1) according to the B2 and A2 emission scenarios. For the future period (2071–2099), the principal effect of water stress is to reduce potential yields almost everywhere in the domain, as moisture availability and evapotranspiration are modelled to be lower.

We next present results for the yield of wheat averaged by country. The total yield (under water-limited conditions) for each country (and period) is calculated first and is then divided by the total number of grid points for each country without considering whether a grid point is suitable or not, to derive the country average yield.

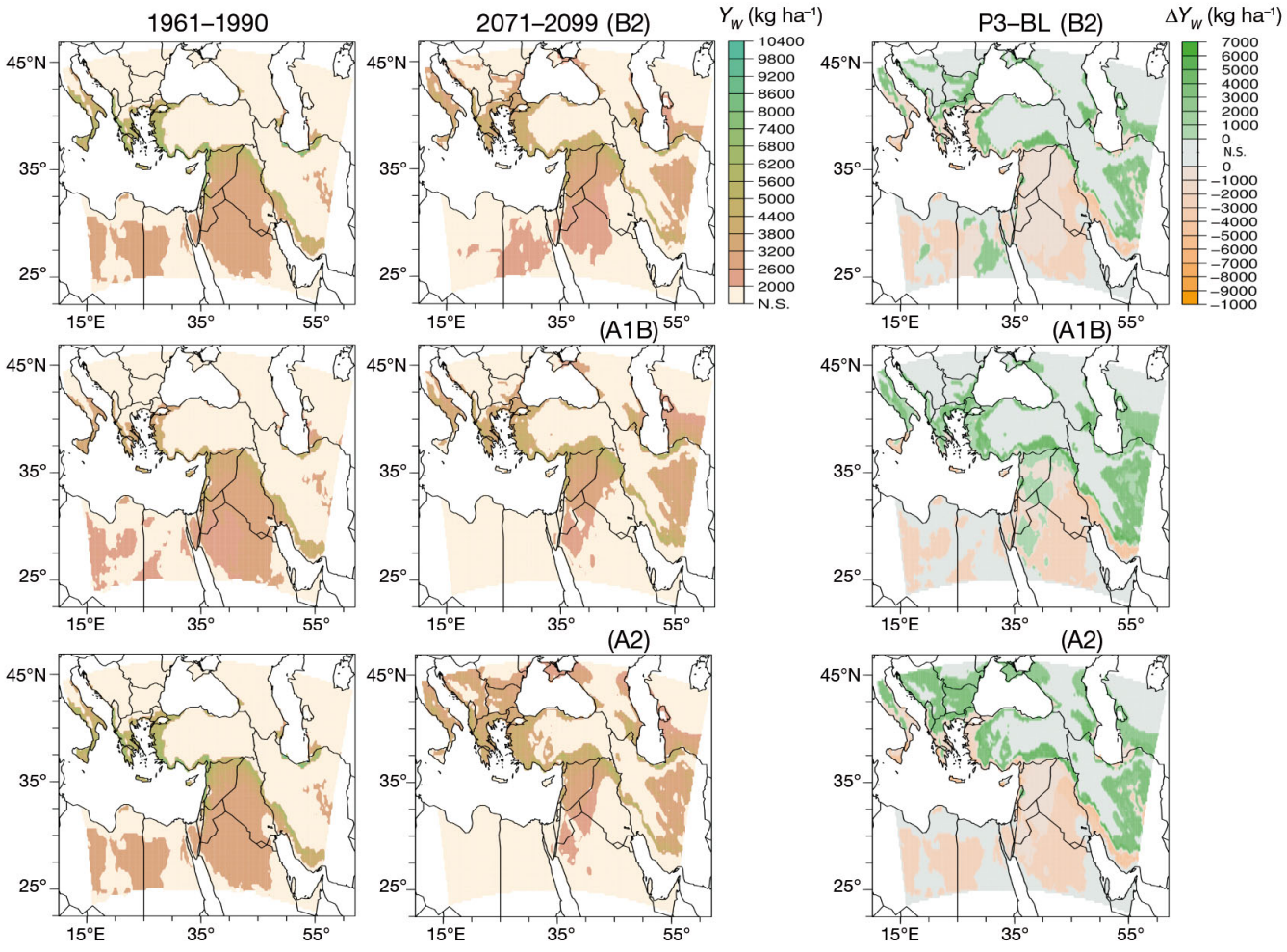

Fig. 6. Water-limited yields (Y_w) of winter (durum) wheat *Triticum tirgidum* in the baseline (BL) period 1961–1990 and in 2071–2099, and projected change (ΔY_w) for the 3 emission scenarios (B2, A1B, A2). N.S.: areas not suitable for durum wheat cultivation

Table 2 shows the actual yields for the period of 1961–1990 as provided by the FAO (for the countries of the EMME region where these are available) as well the derived water-limited yield for durum wheat for the same BL period based on the intermediate A1B scenario. An appropriate conversion factor of 0.875 for winter wheat (provided by GAEZ, 9.2 Model Documentation, Fischer et al. 2012) is applied to the modelled yield estimations, to account for the weight of the modelled product compared to the weight given by FAOSTAT. Even though this factor is applied, a strict comparison between the two, for model evaluation purposes, is not appropriate since: (1) the potential yield calculation assumes that the whole area for each country is available, while the actual yield is documented from the observed production in the fields where it is cultivated; (2) the actual yield numbers may include more types of wheat (not specified in the FAOSTAT records), while in the table we show only the results for durum wheat as the most common type grown in the region; (3) other factors that determine actual production, such as management practices, are not varied (for example we use a fixed crop calendar); (4) the RCM data have not undergone bias correction (due to the lack of long-term, daily observed data for all grid points in the study domain, discussed by Tanarhte et al. 2012). Nevertheless, we derive the difference between the simulated and the actual yields, labelled in the table as 'yield gap', which, according to the above, predominantly depends on the modelled climate. This metric provides insight in the crop yield 'climatic potential' of the region also with regards to the projected climate change, as detailed next.

From inspection of the values in Table 2, we see which countries with favourable climate conditions allow high potential yields, much larger than the actual production (i.e. with high yield gaps). Cyprus,

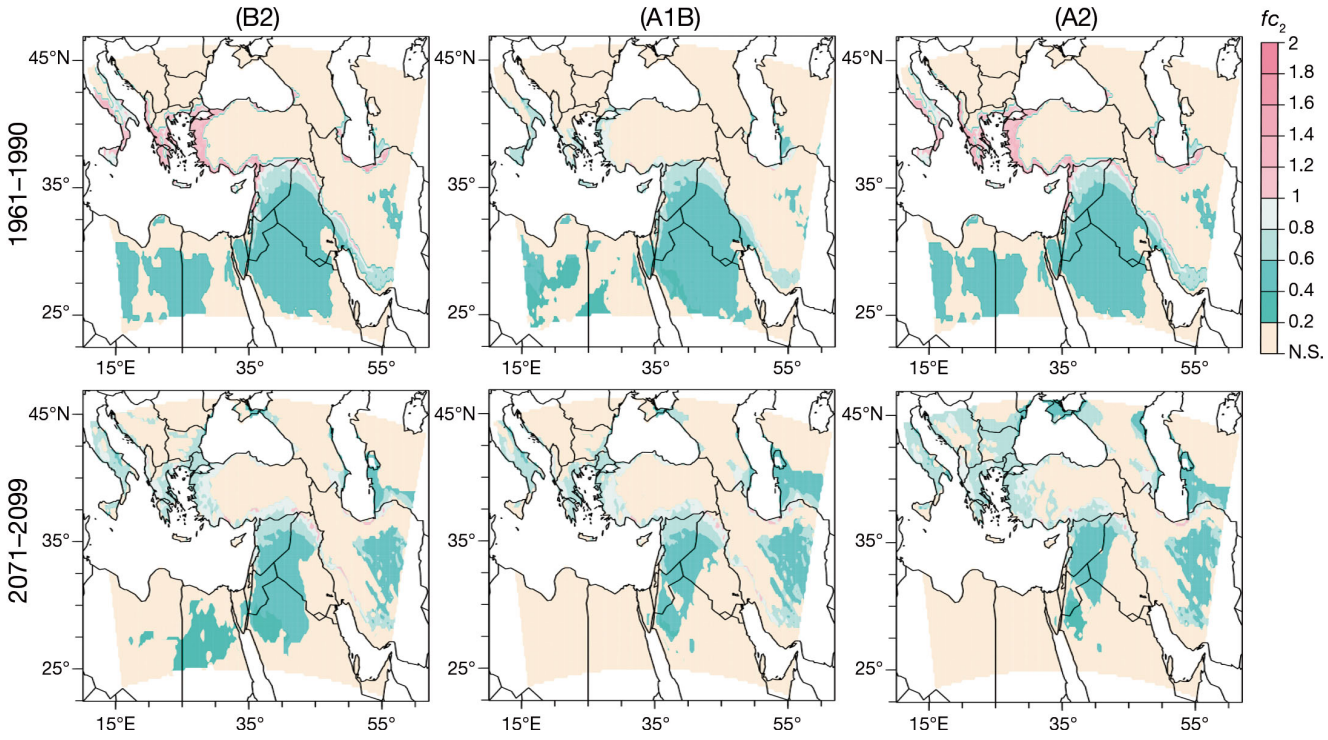

Fig. 7. Water-stress yield-limiting factor fc_2 (calculated as water-limited yield / potential yield, Y_w/Y_p) for the 3 emission scenarios (B2, A1B, A2) and the periods 1961–1990 and 2071–2099. N.S.: not suitable

Lebanon, Syria, Jordan and Iraq climatically have a large potential for higher yields, which could be limited by the projected warming, as by the end of the 21st century, their potential yield is projected to decrease (with the exception of Lebanon and Syria). For the other selected countries (Libya, Israel, Italy, Albania, Bulgaria, Greece, Turkey and Iran) the yield gap is small or negative, indicating optimal production (i.e. high exploitation under the respective climate conditions) with little room for further growth, or perhaps inability of the model climate and methodology assumptions to capture the real conditions. Interestingly, these countries may still have a margin for higher production in the future, as the climate projections suggest gains in the potential yield. Egypt and Saudi Arabia, which also have negative yield gaps (mainly due to irrigation), may face pressures in the achieved yields in the future due to negative changes in potential yield as a result of climate change.

Table 2. Average yield per country in kg ha^{-1} for the baseline (BL) period 1961–1990: actual Y_a_BL (FAO), modelled water-limited yield Y_w_BL (PRECIS) and their difference Y_{gap}_BL. Also shown is the future period 2071–2099: modelled change from 1961–1990 (ΔY_w). The PRECIS values are based on the A1B emission scenario

Country	Y_a_BL	Y_w_BL	Y_{gap}_BL	ΔY_w
Albania	2127	1030	–1097	908
Bulgaria	3293	0	–3293	775
Cyprus	1233	2825	1592	–2522
Egypt	3335	413	–2922	–454
Greece	2152	1593	–559	1123
Iran	930	529	–401	691
Iraq	809	2409	1600	–1056
Israel	2004	2044	40	–2227
Italy	2500	952	–1548	502
Jordan	692	2447	1755	–743
Lebanon	1209	2632	1423	873
Libya	487	509	23	–582
S. Arabia	2403	1340	–1063	–1161
Syria	1039	2932	1893	60
Turkey	1564	565	–999	843

The model projections of water-limited yield change for 2071–2099 are also presented in Fig. 8, for each country under the 3 emission scenarios. Cyprus, Iraq, Libya and Saudi Arabia show negative changes for all 3 scenarios, with the largest reductions simulated under the high-emission scenario A2. Reduced yields for the end of the century are also calculated for Israel, Jordan and Lebanon with the B2 and A2 scenarios, but for the same countries, the moderate A1B scenario indicates higher yields. Egypt and Syria are also projected to have lower yields. The northern part of the study domain, i.e. Albania, Bulgaria, Greece, Iran and Turkey, is projected to have

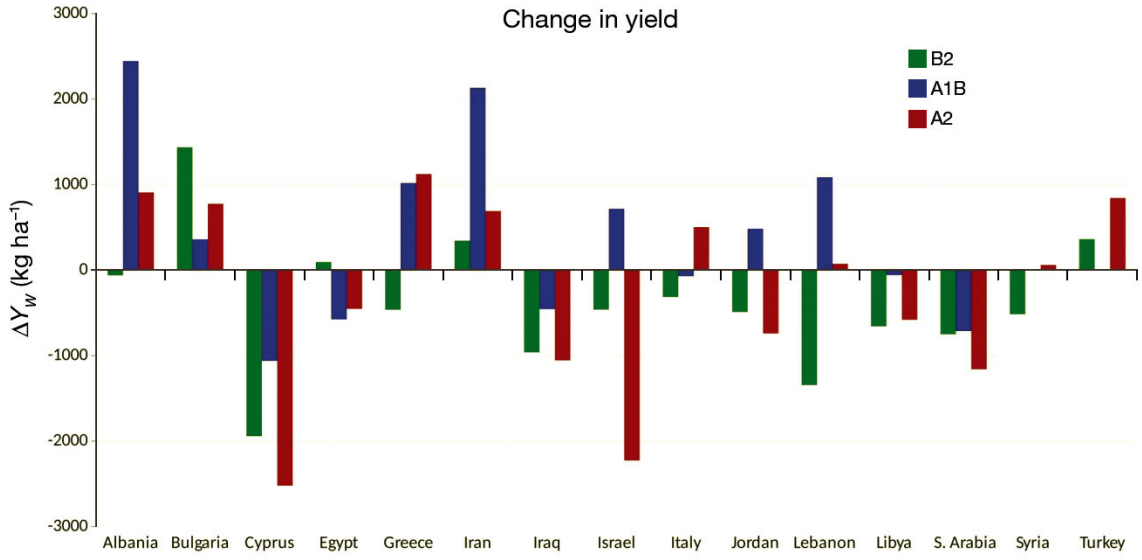

Fig. 8. Country average changes in water-limited yield (Y_w) of winter wheat *Triticum tirgidum* projected in 2071–2099 (P3) compared to the baseline (BL) period 1961–1990 for the 3 emission scenarios (B2: green, A1B: blue, A2: red)

higher yields, especially under the A1B and A2 emission scenarios, where the increasing temperatures bring winter average conditions above the lower cold threshold, as mentioned in the discussion of Fig. 6. On the other hand, it seems that although the B2 scenario is the least severe of the 3 (i.e. with the smallest projected warming), it still induces negative changes to almost all countries in the southern part of the study domain (with the warmest climatic BL). Even the small projected warming in these countries shifts the prevailing temperatures above the upper threshold for optimum growth for winter wheat.

5. DISCUSSION AND CONCLUSIONS

In this study we project changes of potential crop yields of wheat in the EMME region by taking into account changes in temperature, incoming solar radiation and evapotranspiration. Our work complements the GAEZ web portal (www.gaez.iiasa.ac.at/) developed and maintained by FAO and IIASA, since it allows the use of additional gridded climate datasets as input for the crop yield calculations, provided here by simulations with the PRECIS RCM. The crop studied in this paper is winter (durum) wheat, the most important cereal for the region.

Considering the recent 20th century temperature and solar radiation conditions simulated by PRECIS, durum is indeed a high yielding (>4000 kg ha^{-1}) and widespread cultivar in the EMME region, particularly favoured in the Fertile Crescent (from Iraq to Egypt) and the coastal areas of eastern Mediterranean Europe. Future climate conditions, modelled on the basis of 3 IPCC emission scenarios, will cause durum wheat to become less suitable in Libya, Egypt, Saudi Arabia and southern Iraq, as the additional projected heat negatively affects the upper temperature thresholds for optimum crop growth. On the other hand, the future warming in the Balkans and Anatolia with temperatures above the lower optimum thresholds for durum results in higher potential yields.

An analysis of the area average per country reveals that for durum wheat, the high potential for yield improvement (as suggested by our positive yield gap estimates) in Cyprus, Israel, Lebanon, Syria, Jordan and Iraq may be reduced by the end of the century due to climate warming (even under the least intense B2 emission scenario), while the low (or negative) yield gap countries could experience increases in potential yield, mainly under the A1B and A2 scenarios.

The implementation of the GAEZ methodology in this paper lies, in terms of accuracy, in between simple linear relations of yield and temperature and the more complex process-based crop models (Semenov et al. 2012). The assumptions of the applied methodology as well as the specific climate model output may also have affected the calculated yield gaps. Nevertheless, this AEZ approach applied here on RCM data allows the straightforward input of any climate model dataset and demonstrates its utility for regional assessments of climate change impacts on crop yields and food security. Our current analysis does not include the CO_2 fertilization (i.e. the direct effect on

photosynthetic rates; for example, see Kimball et al. 2002, Sakurai et al. 2014) due to the uncertainties of the actual effects (Ainsworth et al. 2008, Koehler et al. 2013). We have also relied on mean climatic conditions; therefore, the potentially important role of climate extremes (Teixeira et al. 2013) is not taken into account. These additional factors associated with climate change will be investigated in a follow-up study, including investigation of adaptation options by adjusting the growth cycle through changes in the crop calendar (i.e. by altering sowing dates).

Acknowledgements. We are grateful to the editor and 2 anonymous reviewers for their comments and suggestions. We acknowledge Harry van Velthuizen at the International Institute for Applied Systems Analysis (IIASA) for his valuable help with the GAEZ manual; and IIASA and FAO for providing the Global Agro-ecological Zones methodology. Material was produced using PRECIS Software provided by the Hadley Centre of the UK Met Office. The research leading to these results has received funding from the European Research Council under the European Union's Seventh Framework Programme (FP7/2007-2013) / ERC grant agreement no. 226144 (C8 Project).

LITERATURE CITED

Ainsworth EA, Leakey ADB, Ort DR, Long SP (2008) FACEing the facts: inconsistencies and interdependence among field, chamber and modeling studies of elevated [CO_2] impacts on crop yield and food supply. New Phytol 179:5–9

Asseng S, Thomas D, McIntosh P, Alves O, Khimashia N (2012) Managing mixed wheat-sheep farms with a seasonal forecast. Agri Sys 113:50–-56

Chenoweth J, Hadjinicolaou P, Bruggeman A, Lelieveld J and others (2011) Impact of climate change on the water resources of the eastern Mediterranean and Middle East region: modeled 21st century changes and implications. Water Resour Res 47:W06506, doi:10.1029/2010WR010269

Ciais P, Reichstein M, Viovy N, Granier A and others (2005) Europe-wide reduction in primary productivity caused by the heat and drought in 2003. Nature 437:529–533

Collins M, Booth B, Harris G, Murphy J, Sexton D, Webb M (2006) Towards quantifying uncertainty in transient climate change. Clim Dyn 27:127–147

de Wit CT (1965) Photosynthesis of leaf canopies. Agricultural Research Reports 663. Pudoc, Wageningen

Fischer G, van Velthuizen H, Shah M, Nachtergaele F (2002) Global agro-ecological assessment for agriculture in the 21st century: methodology and results. IIASA Research Report RR-02. International Institute for Applied Systems Analysis, Laxenburg

Fischer G, Nachtergaele FO, Prieler S, Teixeira E and others (2012) Global Agro-Ecological Zones (GAEZ v3.0) – model documentation. IIASA, Laxenburg, and FAO, Rome. Available at www.gaez.iiasa.ac.at/docs/GAEZ_Model_Documentation.pdf

Grasso M, Feola G (2012) Mediterranean agriculture under climate change: adaptive capacity, adaptation, and ethics. Reg Environ Change 12:607–618

Habash DZ, Kehel Z, Nachit M (2009) Genomic approaches for designing durum wheat ready for climate change with a focus on drought. J Exp Bot 60:2805–2815

ICARDA (International Center for Agricultural Research in the Dry Areas) (2001) Spain and ICARDA. Ties that bind, No. 14. ICARDA, Aleppo

Iglesias A, Rosenzweig C, Pereira D (2000) Agricultural impacts of climate change in Spain: developing tools for a spatial analysis. Glob Environ Change 10:69–80

Iizumi T, Luo JJ, Challinor AJ, Sakurai G and others (2014) Impacts of El Niño Southern Oscillation on the global yields of major crops. Nat Commun 5:3712

Kassam AH (1977) Net biomass production and yield of crops. FAO, Rome

Key JM (2005) Wheat: its concept, evolution, and taxonomy. In: Royo C, Nachit MM, Di Fonzo N, Araus JL, Pfeiffer WH, Slafer GA (eds) Durum wheat breeding: current approaches and future strategies, Vol 1. Food Products Press, an imprint of the Haworth Press Inc, New York, NY, p 3–61

Kimball B, Kobayashi AK, Bindi M (2002) Responses of agricultural crops to free-air CO_2 enrichment. Adv Agron 77: 293–368

Koehler AK, Challinor AJ, Hawkins E, Asseng S (2013) Influences of increasing temperature on Indian wheat: quantifying limits to predictability. Environ Res Lett 8: 034016, doi:10.1088/1748-9326/8/3/034016

Leff B, Ramankutty N, Foley J (2004) Geographic distribution of major crops across the world. Global Biogeochem Cycles 18:GB1009, doi:10.1029/2003GB002108

Lelieveld J, Hadjinicolaou P, Kostopoulou E, Chenoweth J and others (2012) Climate change and impacts in the eastern Mediterranean and the Middle East. Clim Change 114:667–687

Lidon FC, Almeida AS, Leitao AL, Silva MM, Pinheiro N, Macas B, Costa R (2014) A synoptic overview of durum wheat production in the Mediterranean region and processing following the European Union requirements. Emir J Food Agric 26:693–705

Luo Q (2011) Temperature thresholds and crop production: a review. Clim Change 109:583–598

Moriondo M, Giannakopoulos C, Bindi M (2011) Climate change impact assessment: the role of climate extremes in crop yield simulation. Clim Change 104:679–701

Nachit MM, Elouafi I (2004) Durum adaptation in the Mediterranean dryland: breeding, stress physiology, and molecular markers. In: Rao SC, Ryan J (eds) Challenges and strategies for dryland agriculture. CSSA Special Publication 32. Crop Science Society of America Inc., American Society of Agronomy Inc, Madison, WI, p 203–218

Nakicenovic N, Davidson O, Davis G, Grübler A and others (2000) Special report on emissions scenarios. A special report of Working Group III of the Intergovernmental Panel on Climate Change. Cambridge University Press, Cambridge

Naresh Kumar S, Aggarwal PK, Swaroopa Rani DN, Saxena R, Chauhan N, Jain S (2014) Vulnerability of wheat production to climate change in India. Clim Res 59:173–187

Oldeman LR, Frére M (1982) A study of the agroclimatology of the humid tropics of South-East Asia. Tech Note 179. WMO, Geneva

Olesen JE, Bindi M (2002) Consequences of climate change for European agricultural productivity, land use and policy. Eur J Agron 16:239–262

Rivero Vega RE (2008) Workbook of climate change impact assessment in agriculture. Basic knowledge, methodology and tools. Camagüey Meteorological Centre. Available at http://www.agrometeorology.org/files-folder/repository/INSAMRogerWorkbookadaptclimchange.pdf

Rosenzweig C, Jones JW, Hatfield JL, Ruane AC and others (2013) The Agricultural Model Intercomparison and Improvement Project (AgMIP): protocols and pilot studies. Agric For Meteorol 170:166–182

Rosenzweig C, Elliott J, Deryng D, Ruane AC and others (2014) Assessing agricultural risks of climate change in the 21st century in a global gridded crop model intercomparison. Proc Natl Acad Sci USA 111:3268–3273

Sacks JW, Deryng D, Foley J, Ramankutty N (2010) Crop planting dates: an analysis of global patterns. Glob Ecol Biogeogr 19:607–620

Sakurai G, Iizumi T, Nishimori M, Yokozawa M (2014) How much has the increase in atmospheric CO_2 directly affected past soybean production? Sci Rep 4:4978, doi: 10.1038/srep04978

Semenov MA, Mitchell RAC, Whitmore AP, Hawkesford MJ, Parry MAJ, Shewry PR (2012) Shortcomings in wheat yield predictions. Nat Clim Change 2:380–382

Sen B, Topcu S, Türke M, Sen B, Warner JF (2012) Projecting climate change, drought conditions and crop productivity in Turkey. Clim Res 52:175–191

Shewry PM, Underwood C, Wan Y, Lovegrove A and others (2009) Storage product synthesis and accumulation in developing grains of wheat. J Cereal Sci 50:106–112

Tanarhte M, Hadjinicolaou P, Lelieveld J (2012) Intercomparison of temperature and precipitation data sets based on observations in the Mediterranean and the Middle East. J Geophys Res 117:D12102, doi: 10.1029/2011JD017293

Teixeira EI, Fischer G, van Velthuizen H, Walter C, Ewert F (2013) Global hot-spots of heat stress on agricultural crops due to climate change. Agric For Meteorol 170:206–215

Van Ittersum M, Cassman KG, Grassini P, Wolf J, Tittonell P, Hochman Z (2013) Yield gap analysis with local to global relevance — a review. Field Crops Res 143:4–17

Van Wart J, van Bussel LGJ, Wolf J, Licker R and others (2013) Use of agro-climatic zones to upscale simulated crop yield potential. Field Crops Res 143:44–45

Vanuytrecht E, Raes D, Willems P, Semenov MA (2014) Comparing climate change impacts on cereals based on CMIP3 and EU-ENSEMBLES climate scenarios. Agric For Meteorol 195–196:12–23

Zittis G (2015) Regional climate modelling in the eastern Mediterranean and the Middle East: aspects of summer warming and related feedbacks under a changing climate. PhD thesis, The Cyprus Institute, Nicosia. doi: 10.13140/RG.2.1.4698.3845

Zittis G, Hadjinicolaou P, Lelieveld J (2014) Role of soil moisture in the amplification of climate warming in the eastern Mediterranean and the Middle East. Clim Res 59:27–37

Zittis G, Hadjinicolaou P, Fnais M, Lelieveld J (2015) Projected changes in heat wave characteristics in the eastern Mediterranean and the Middle East. Reg Environ Change 1–14, doi:10.1007/s10113-014-0753-2

Appendix 1. Temperature profiles and requirements

Temperature profiles are defined in terms of 9 classes of 'temperature ranges', listed in Table A1 for days with average (mean) temperature <–5°C to >30°C, at 5°C intervals, in combination with distinguishing increasing and decreasing temperature trends within the averaged 30 yr period.

Table A1. Temperature profile classes

Average temperature (°C)	Growth cycle duration (d)	Temperature trend Increasing	Decreasing
>30	L1	*L*1a	*L*1b
30–25	L2	*L*2a	*L*2b
25–20	L3	*L*3a	*L*3b
20–15	L4	*L*4a	*L*4b
15–10	L5	*L*5a	*L*5b
10–5	L6	*L*6a	*L*6b
5–0	L7	*L*7a	*L*7b
0 to –5	L8	*L*8a	*L*8b
< –5	L9	*L*9a	*L*9b

Temperature profiling is firstly performed on the prevailing average temperature conditions of each grid box. These prevailing temperature profile conditions are then tested against the crop temperature requirements (found in Table 1 of the main text) for matching.

Temperature profile requirements are crop-specific rules that take into account the temperature profile classes shown in Table A1. GAEZ has defined in detail the temperature profile requirements for each crop; Table 1 shows the corresponding requirements for winter wheat. These are the 2 data sets for optimum and sub-optimum conditions that are needed to be satisfied in order for a grid box to be considered suitable for cultivation of winter wheat; otherwise the grid boxes are marked as non-suitable.

Appendix 2. Biomass and yield calculation

All equations of the biomass and yield calculation model (AEZ methodology) (Kassam 1977, Fischer et al. 2012) are described in detail in the following paragraphs.

The maximum rate of gross biomass production (b_{gm}) is related to the maximum net rate of CO_2 exchange of leaves (P_m), which is dependent on temperature, the photosynthesis pathway of the crop and the level of atmospheric CO_2 concentration.

$$b_{gm} = F \times b_0 + (1 - F) \quad \text{(A1)}$$

where F is the fraction of daytime during which the sky is clouded and is related to the maximum active incoming shortwave radiation on clear days (A_c or photosynthetically active radiation, PAR; de Wit 1965) and the incoming shortwave radiation (SWR) which is provided by the PRECIS RCM (units for both is [cal cm^{-2} d^{-1}]). b_0 is the gross dry matter production rate of a standard crop for a given location and time of the year on a completely overcast day, and b_c is the gross dry matter production rate of a standard crop for a given location and time of the year on a perfectly clear day, both measured in kg ha^{-1} d^{-1} (de Wit 1965). A_c, b_0 and b_c are interpolated from Vega (2008).

The net biomass production B_n for a crop of N days, where half of the maximum rate of net biomass (dry matter) production is the seasonal average rate of net biomass production, can be derived from:

$$B_n = \frac{0.36 b_{\mathrm{gm}} \times L}{\frac{1}{N} + 0.25 c_t} \quad \text{(A2)}$$

where b_{gm} is the maximum rate of gross biomass production and is calculated by Eq. (A1), L is the growth ratio of b_{gm} at the actual leaf area index (LAI) to b_{gm} at an LAI of 5, N is the duration of the normal growth cycle, and c_t is the maintenance respiration, dependent on both crop and temperature.

Finally, potential yield (Y_p) is estimated from net biomass (B_n) using the equation:

$$Y_p = H_i \times B_n \quad \text{(A3)}$$

where H_i is the harvest index, i.e. the proportion of the net biomass of a crop that is economically useful.

Yield reduction in response to water deficits is then calculated as a function of the relationship between actual crop evapotranspiration (ΣET_a, mm d^{-1}) and maximum crop evapotranspiration (ΣET_m, mm d^{-1}), both accumulated within the 4 crop stages. Result of this calculation is a water stress yield reduction factor (fc_2), using the following equations:

$$fc_2^T = 1 - k_y 0 \times \left(1 - \frac{\sum_1^{TCL} ET_a}{\sum_1^{TCL} ET_m} \right) \quad \text{(A4)}$$

fc_2^T is the effect of overall deficit, k_y0 is an average value of the water stress coefficient for the overall crop growth cycle, which expresses the sensitivity of specific crop to water stress, ET_a is the actual crop evapotranspiration, and ET_m is the maximum crop evapotranspiration (mm d^{-1}).

$$fc_2^{CS} = \prod_{j=1}^{4} \left(1 - ky_j \times \left(1 - \frac{TETa_j}{TETm_j} \right) \right)^{\lambda_j} \quad \text{(A5)}$$

fc_2^{CS} represents the weighted effect of crop-stage specific water stress, k_y is the crop-specific value of the water stress coefficient for each crop development stage (j = 1–4; initial, vegetative, reproductive, maturation). TET_a and TET_m are respectively total actual evapotranspiration and total maximum crop evapotranspiration for days during each crop growth stage. λj are weighting coefficients, the sum of which equals 1, and are taken as the relative length of each crop development stage.

$$fc_2 = \min\left(fc_2^{CS}, fc_2^T\right) \quad \text{(A6)}$$

where fc_2 is the water-stress reduction factor.

Water-limited yield (Y_w) is then calculated as potential yield (Y_p) multiplied by the water-stress reduction factor fc_2 by the following equation:

$$Y_w = Y_p \times fc_2 \quad \text{(A7)}$$

Editorial responsibility: Toshichika Iizumi, Tsukuba, Japan

Submitted: October 16, 2014; Accepted: April 7, 2016
Proofs received from author(s): June 3, 2016